

3D Printed Polymer Scaffolds for Bone Tissue Regeneration

Nipun U. Jayatissa¹, Sarit Bhaduri²

¹ Maumee Valley Country Day School, 1715 South Reynolds Road, Toledo, Ohio 43614-1499

² University of Toledo, Department of Mechanical Engineering and Surgery, 2801 W. Bancroft Street, Toledo, Ohio 43606

SUMMARY

The regeneration of bone defects is a significant clinical challenge for patients around the world. The ideal scaffolds for bone tissue repair should provide biocompatibility, pore architecture, biodegradability, mechanical support, and cell attachment sites. Conventionally fabricated polymer scaffolds are still unable to make ideal scaffolds for bone tissue repair due to the lack of all the above mentioned properties. The investigated hypothesis was that increasing pore sizes of the scaffolds would cause an increase in the porosity and a decrease in the compressive modulus. In order to test the hypothesis, we designed three different pore sizes (200, 400, and 800 μm) in three different scaffolds using computer software. Relatively new 3D printing technology was used to print the three different types of porous scaffolds using polycaprolactone (PCL) polymer. These scaffolds were characterized for percent porosity, pore architecture, morphology, mechanical properties, and evaluated for biocompatibility and cell attachment with murine pre-osteoblasts. The percent porosity of these scaffolds (n=7) significantly increased from 13.31 to 61.66 (p<0.001) with the increase in pore size. The average compressive modulus of scaffolds (n=7) significantly decreased with the increase in pore size (p<0.001). The averaged compressive modulus of scaffolds with 200, 400, and 800 μm pores is 82.98 ± 2.02 , 61.60 ± 2.59 , and 47.16 ± 1.73 MPa, respectively. In addition, PCL scaffolds show biocompatibility as determined by an *in vitro* cell study. These results have shown that the hypothesis is validated, and these 3D printed porous PCL scaffolds can be potentially used for bone regeneration applications. response teams and in developing areas.

INTRODUCTION

The replacement or restoration of bone defects caused by trauma, fracture, and disease is a significant clinical challenge for both military and civilian patients (1-3). The bone has an intrinsic capacity to repair itself, which is best observed in the healing of bone fractures (4). However, when bone defects occur as a result of severe injury, healing may not commence spontaneously. Complicated pathological fractures or large defects need to be bridged using external intervention (5,6). Annually, the cost for bone fracture repair exceeds \$19 billion, and annual fractures and costs are projected to increase by 50% in 2025 (7).

There are two main types of bone grafts used in bone

fracture repair: autografts and allografts (8,9). These grafts provide the necessary mechanical and structural support during bone healing. Autograft bone tissue is taken from the patient's own healthy bone and implanted at the fractured site. Autograft contains viable cells, including new bone forming osteoblasts, supports the stability of the fractured site, and supports osteoblast function. However, the harvest site of autograft is subjected to injury due to the removal of the graft, and the patient undergoes donor site morbidity such as blood loss, infection risk, and scar formation. Allograft is taken from a cadaver and supports mechanical stability at the defect site and allows for cell attachment and cell function for surrounding cells (10). The two clinical drawbacks of the allograft are immunologic mismatch and risk of transmission of viral diseases.

Because of these clinical issues, scientists seek better methods for bone fracture healing, thus bone tissue engineering has emerged as a solution to treat bone fractures effectively and safely (11). In bone tissue engineering, one of the key elements is to create a resorbable or degradable scaffold, made of polymers, ceramics or polymer-ceramic composites (12), and bioactive glass (bioglass) (13,14). Bioglass has shown osteoconductivity, allows cells to attach to the surface of a material and promotes cell function. Bioglass has shown better osteoconductivity and therefore, polymer composite with bioglass have enhanced osteoconductivity compared to polymers alone. However, compared to polymers, the main drawback of bioglass is its inherent brittleness. Therefore, bioglass with polymer composite is used to prepare the scaffolds for bone regeneration to improve flexibility and reduce brittleness.

Scaffolds are three-dimensional (3D), biocompatible, and porous structures, which can mimic the extracellular matrix (ECM) properties including mechanical support, cellular activity, and protein production through biochemical and mechanical interactions. Bone is a load-bearing tissue, and in everyday life, compressive loading is the most common type of loading applied to bone (15). Therefore, it is important to know the compressive mechanical properties of scaffolds such as the compressive modulus. The ratio of applied compressive stress (force) to strain in the linear region is called compressive modulus (or stiffness). In addition, scaffolds provide sites for cell attachment, proliferation, differentiation, and stimulates bone tissue formation *in vivo* (12,16).

Pores in the scaffold are important for vascularization

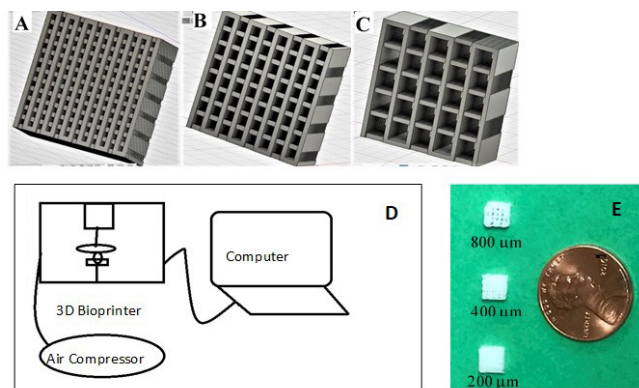


Figure 1. Cuboidal shaped porous PCL scaffold design created by computer software with three different pore sizes. (A) 200 μm , (B) 400 μm , (C) 800 μm . (D) Sketch of 3D printing of scaffolds. (E) A picture shows visual appearance of printed PCL scaffolds with different pore sizes.

in vivo, which enables the transport of nutrients and waste-products in and out of the bone (6). Pore size and porosity are vital properties of a biomaterial scaffold for bone tissue regeneration, and large pore sizes and high porosity seems to enhance the *in vivo* bone ingrowth and osseointegration of the implant (17). The minimum recommended pore size for a scaffold should be between 100 and 150 μm (6,17), but other studies have observed better osteogenesis when implants have larger than 300 μm pore sizes. However, the increase in scaffold pore size results in reduced mechanical integrity of the scaffold.

Conventional polymer scaffolds are still unable to make ideal scaffolds for bone repair due to its poor mechanical properties, quick biodegradation, and inherent toxicity (18,19). In addition, current fabrication methods for polymer scaffolds use organic solvents, salts, and secondary containers to create the pores of the scaffolds. These additional materials may contribute contamination of the polymer scaffolds (12).

Relatively new 3D printing technology has emerged as a promising tool to fabricate patient specific 3D scaffolds with precise features since conventional scaffolds are unable to make ideal scaffolds for bone regeneration (18,19). This technology provides advantages compared to conventional fabrication methods including fabrication of versatile scaffolds with complex shapes, capability for homogeneous cell distribution, and mimicry of the ECM. 3D printing technology allows complex shapes of scaffolds to be printed with a bioink directly from a computer aided design (CAD) file. This technology is a branch of additive manufacturing which involves the process of sequentially adding layer upon layer of materials (12).

We investigated the hypothesis that increasing the pore size of the scaffolds would cause an increase in the porosity and a decrease in the compressive modulus. In this study, melted polycaprolactone (PCL) was used as a bioink to print the 3D porous scaffolds with a computer-controlled layer-by-layer addition process using extrusion printing. PCL is thermoplastic polyester and melts at 58-60°C. PCL degrades

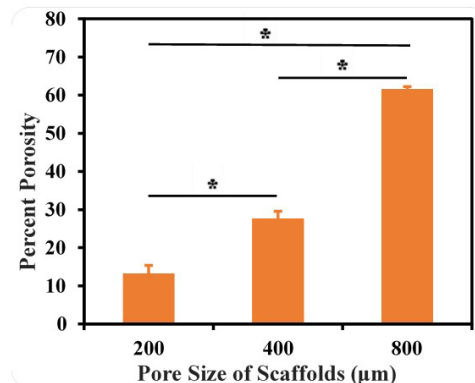


Figure 2. Percent porosity for three different porous PCL scaffolds. * shows the statistically significant difference. Error bars represent the standard error of the data.

at a slower rate and is non-toxic. The Food and Drug Administration (FDA) approved the use of PCL related medical products such as sutures containing PCL and implantable contraceptive device (Capronor) (20). The use of PCL for drug delivery applications has also been approved by the FDA (21). To test the hypothesis, this paper focuses on the design and printing of 3D scaffolds with three different pore sizes (200 μm , 400 μm , and 800 μm); the characterization of scaffolds in terms of percent porosity, morphology, and mechanical properties; and the evaluation of scaffolds for cell (murine pre-osteoblast) viability, attachment, and proliferation.

RESULTS

Design and Printing of Scaffolds

To test the hypothesis, we made three different porous scaffold designs with the same dimensions and three different pore sizes (200, 400, and 800 μm) using computer software (Figure 1A-C). The scaffolds with 200, 400, and 800 μm pore sizes took 25, 20, and 15 min, respectively, to completely print individually. The scaffold with small pores has more struts than the other two types of scaffold; therefore, it takes a longer time to print. Figure 1D shows the schematic representation of 3D printing the scaffolds, and Figure 1E shows the visual appearance of all three types of printed scaffold. The printed scaffolds all have the cuboidal shape similar to the original computer design of scaffolds (Figure 1D) with the same length (5 mm), width (5 mm), and thickness (2.4 mm).

Percent Porosity of Scaffolds

The impact of different pore sizes on scaffold porosity was determined by calculating the percent porosity of the scaffolds. The numbers of pores in the scaffold increased with decreasing pore size. Scaffolds with 200, 400, and 800 μm pores showed an average percent porosity ($n=7$) of 13.31 \pm 2.06, 27.69 \pm 1.85, and 61.66 \pm 0.62, respectively (Figure 2). The percent porosity of scaffold significantly increased ($p<0.001$) with the increase in pore size. The percent porosity of each group of scaffolds was significantly different ($p<0.001$) when compared with the other two scaffold groups.

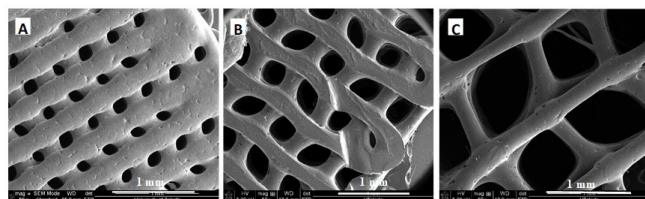


Figure 3. SEM images of three different porous PCL scaffolds. (A) 200 μm pores, (B) 400 μm pores, (C) 800 μm pores. Scale: 1 mm.

Morphology of Scaffolds with SEM

The surface and pore morphology of scaffolds with different pore sizes were studied with SEM images (Figure 3). The images confirmed that the actual measured pore size of the scaffold increased with the designed increase in pore size. The original computer design of the scaffolds has square shaped pores in each type of scaffold groups. The pore morphology of 3D printed scaffolds with 400 and 800 mm pore sizes were approximately similar to the original cubical computer design. However, slightly smaller pore sizes were observed for scaffolds with original pore sizes of 200 and 400 mm. In addition, the struts of all three types of scaffolds were not straight as the original design.

Mechanical Properties of Scaffolds

To test how different pore sizes impact the compressive modulus, the scaffolds were measured for mechanical properties. The stress-strain graph was generated for 200 μm pore scaffold, and the linear region was used to calculate the compressive modulus of the scaffold (Figure 4). The mean and standard error of the compressive modulus of the scaffolds are plotted in Figure 5. The average compressive modulus of the scaffolds ($n=7$) significantly decreased with the increase in pore size of the scaffold ($p<0.001$). We calculated the average compressive modulus for scaffolds with 200, 400

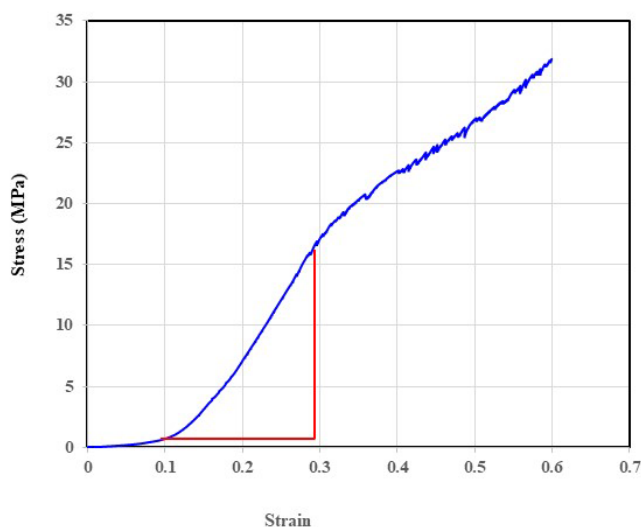


Figure 4. Stress-Strain plot for PCL scaffold used to calculate the compressive modulus. The slope was calculated using the distances in red in linear region.

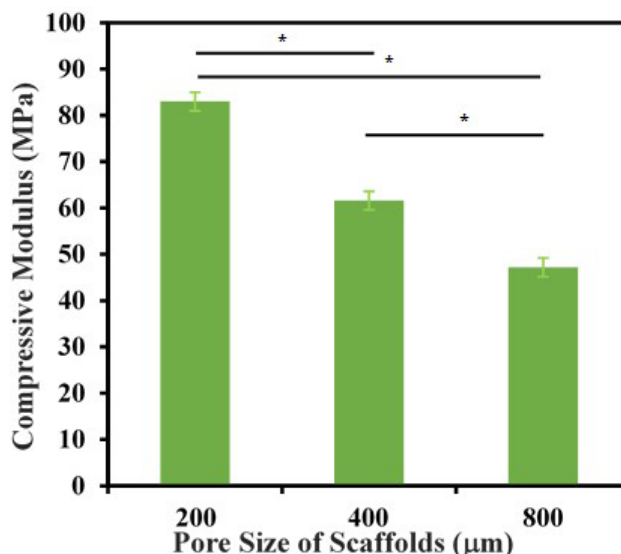


Figure 5. Compressive modulus for PCL scaffolds with three different pore sizes. * shows the statistically significant difference. Error bars represent the standard error of the data.

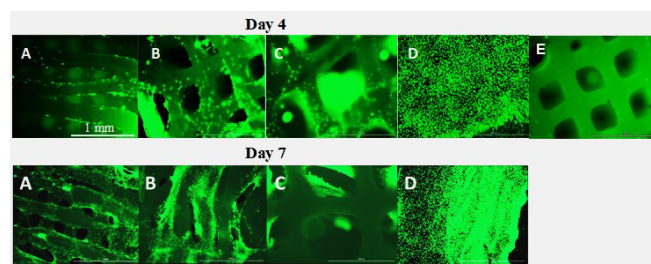


Figure 6. Fluorescent images for pre-osteoblasts cultured on PCL scaffolds at days 4 and 7 with three different pore sizes. (A) 200 μm , (B) 400 μm , (C) 800 μm , (D) control (without scaffold), (E) negative control image of a scaffold without cells. Scale: 1 mm.

and 800 μm pores to be 82.98 ± 2.02 , 61.60 ± 2.59 , and 47.16 ± 1.73 MPa, respectively. The compressive modulus of each scaffold types showed a significant difference ($p<0.001$) when compared to the two other types of scaffold.

Cell Culture Studies In Vitro

The 3D printed scaffolds were qualitatively evaluated for cell attachment and viability using pre-osteoblasts at days 4 and 7 after cell seeding by visualizing cell attachment to the scaffolds (Figure 6). This result suggested that 3D printed PCL scaffolds permit cell attachment at days 4 or 7.

DISCUSSION

The investigated hypothesis was that increasing the pore size of the scaffolds would cause an increase of the porosity and a decrease of the compressive modulus. In this study, 3D porous PCL scaffolds were designed with three different pore sizes (200, 400, and 800 μm) and directly printed using a melt extrusion 3D printing technique. The shape, size, and pore design of the 3D printed scaffolds (Figure 1E) were quite similar to the original designs. This technique of direct printing

did not require the use of organic solvents or salts to create the pores of the scaffolds. Therefore, this direct printing of PCL scaffolds avoids any possible contamination with any other secondary material or organic solvents.

The average percent porosity of the scaffolds significantly increased ($p < 0.001$) with the increase in pore size of the scaffolds, so we accept our hypothesis (**Figure 2**). The percent porosity ranged from approximately 13.31 to 61.66 for the three types of scaffold. In this study, the pores of the PCL scaffolds were designed to mimic the natural human bone. The porosity of cortical bone and trabecular bone is in the range of 5% to 30% and 30% to 90%, respectively. Therefore, based on the results of the PCL scaffolds, they can be used to mimic either type of bone porosity.

The compressive modulus significantly decreased ($p < 0.001$) with the increase in pore size of the scaffold. The average compressive modulus of the three types of PCL scaffolds ranged from 82.98 to 47.16 MPa (**Figure 5F**). The scaffolds with percent porosity of 13.31, 27.69, and 61.66 showed compressive moduli of 82.98, 61.6, and 47.16, respectively. Increasing the pore size of scaffolds reduced the compressive modulus, supporting the hypothesis. Previous studies have shown that the compressive modulus of PCL scaffolds with designed porosity between 37 and 55% is 52 to 68 MPa (22). Another study has shown that the compressive modulus of PCL is 6 MPa for PCL scaffolds with 55% porosity (23). Therefore, the compressive modulus of PCL scaffolds in this study is similar or higher compared to the reported values of previous studies (22). However, the porosity and compressive modulus of the scaffold should be balanced in order to have structurally strong scaffolds to serve for bone repair (24). The compressive modulus of cancellous bone is between 1-5000 MPa (25). Therefore, the PCL scaffolds printed in this study are potentially suitable to use for trabecular bone tissue regeneration.

PCL has shown minimal immune response when PCL devices were implanted for different medical applications (26,27). In addition, PCL devices have been approved by the FDA for medical applications (20). In vitro biocompatibility or cytotoxicity of materials can be evaluated using cell culture studies (28). In this study, cell attachment to the PCL scaffolds was used to determine whether cells were viable with all types of scaffolds (**Figure 6**). Previous studies have suggested that scaffolds with pore sizes in the range of 150-350 μm are optimal for new bone formation, and pores larger than 400 μm are favorable for vascularization (24). Based on the results, the scaffolds with 400 μm pores would be better for future in vivo studies since these scaffolds have good mechanical properties and have large enough pores for cell growth. Although a test for scaffold degradation was not conducted in this study, the total degradation of PCL is reported to be 1.5-2 years (29). The degradation of PCL scaffolds can be accelerated with the increase of porosity in the scaffold. PCL degrades slowly in the body, allowing more structural support for growing cells for a longer period of time until dense tissue

forms. Another advantage of using PCL is that there are no adverse effects of their degraded products which feed into metabolic pathways (21).

The square-shaped pores and straight struts were designed in our original scaffold design. The scaffolds were printed using a computer design, thus theoretically scaffolds should be similar to each other. However, the SEM images showed slight differences in the measured dimensions of the pores as well as slight distortion of the shape of pores and straight lines. Particularly with the small pores, 200 μm , this distortion was highly visible, and pores were slightly small when compared to the computer design's pore sizes in the scaffolds (**Figure 3**). This problem probably arises due to the lack of completely drying of the previously laid layer. Therefore, the new layer was laid down on to the previous layer distorted (or expanded), thus causing distortions. This problem could be avoided by drying the PCL layers as quickly as possible using a dryer or fan before adding the next layer. In this study, square-shaped pores were used. However, changing the pore geometry can be done by modifying the scaffold design; therefore, a scaffold could have squares or ovals. Modifying the shapes could have some impact on the porosity, mechanical properties, and/or cell function. In addition, the quantitative measurement of cell proliferation on the scaffolds can be assessed in the future using the MTS cell proliferation assay.

In conclusion, pre-designed PCL scaffolds with three different pore sizes were directly printed using a 3D printer. The printed scaffolds have shown the increased percent porosity with the increase in pore size of the scaffold. The compressive modulus of the three types of scaffolds increased with the decrease in the pore size of the scaffold. These results show that the hypothesis of this study is supported. In addition, these scaffolds permitted cell attachment as determined by cell culture studies at day 4 and day 7. These scaffolds have shown the reproducibility, biocompatibility, pore interconnectivity, porosity similar to bone, and compressive modulus similar to bone, and we observed viable cells on the scaffolds. Therefore, these PCL scaffolds can be potentially used to regenerate or repair bone defects.

MATERIALS AND METHODS

Materials

PCL Pellets (molecular weight 50,000 Da) were purchased from BioBiotics Inc. (USA). Alpha minimum essential medium (α -MEM), phosphate buffered saline (PBS), penicillin/streptomycin and fetal bovine serum (FBS), and 0.25% trypsin-EDTA phenol red were all purchased from Gibco (USA). Live/dead cell viability/cytotoxicity kit were purchased from Invitrogen (USA).

Design and Printing of 3D Porous PCL Scaffolds

Three different types of 3D porous scaffolds with pore sizes 200, 400, and 800 μm were designed and drawn using

Autodesk Fusion 360 software (**Figure 1A**). The dimensions of these cuboid 3D scaffolds were designed with a length of 5 mm, a width of 5 mm, and a thickness of 2.2 mm. Each scaffold was designed to have 22 layers with 100 μm thickness of each layer in the z direction. A commercial bioprinter, BioBots (BioBots Inc., Philadelphia, PA, USA) with computer driven x-y-z moving system attached nozzles was used to print 3D scaffolds by extrusion printing with layer-by-layer process. An air compressor was attached to regulate the pressure of the extruded bioink in the printing system. The PCL pellets were loaded into the metal syringe attached to extruder and melted at 100°C with pressure at 100 PSI.

Percent Porosity of Scaffolds

The total volume of each of the three types of cuboid shaped scaffolds (Total volume = length x width x thickness) was calculated by measuring the length, width, and thickness of each scaffold using a Vernier caliper (n=7). The volume of solids of each scaffold was calculated by measuring the mass of each group of scaffolds (n=7) and dividing it by the density of PCL (1.1 g/cm³). The percent porosity of scaffolds (n=7) from each of the three types of scaffold groups was calculated using the following equation:

$$\text{Percent Porosity} = \left(\frac{\text{Volume of Pores}}{\text{Total Volume}} \right) \times 100\% = \left(\frac{\text{Total Volume} - \text{Volume of Solids}}{\text{Total Volume}} \right) \times 100\%$$

Morphology of Scaffolds with Scanning Electron Microscope (SEM)

The surface and pore morphology of scaffolds (n=3) were observed using SEM (FEI quanta 3D FEG, FEI Company, Hillsboro, OR, USA). Since PCL is not conductive, scaffolds were sputter coated with gold for 30 seconds using a sputter coater.

Test of Mechanical Properties of Scaffolds

The mechanical properties of the scaffolds were conducted using ADMET eXpert 2600 series (ADMET, Inc., Norwood, MA, USA) Universal mechanical testing machine. One scaffold was placed on the middle of the flat smooth steel fixture. Scaffolds from each group (n=7) were compressed by the flat stainless steel crosshead with Interface SM-250 load cell with the rate of 0.01 mm/s. Force on the load transducer against crosshead position graph was generated by ADMET's MTESTQuatro software. Then these data were used to produce stress-strain graph in excel file. Stress and strain of scaffold can be defined as follows:

Stress = Force/bottom or top surface area of the scaffold

Strain = Change of thickness in z-direction/original thickness of the scaffold

The compressive modulus of the scaffold was calculated from the slope of the linear region (elastic region) of the stress-strain graph, for each of the three types of scaffolds.

Cell Culture Studies In Vitro

PCL scaffolds (n=3 per each type of scaffold) were

sterilized with Ultra Violet (UV) light for 30 min in 24-well plate. Next, murine pre-osteoblasts (Sigma) were seeded on top of the scaffolds with cell density of 40,000 cells/well using a medium of alpha minimum essential medium (α -MEM) combined with 15% fetal bovine serum (FBS) and 1% penicillin/streptomycin. The pre-osteoblasts seeded scaffolds in 24-well plate were incubated in 5% CO₂/95% air incubator at 37°C. Culture medium was changed every 2-3 days until scaffolds were used for the testing at day 4 and 7. Another 24-well plate without scaffold was seeded with the cell density of 40,000/well and used as a control (n=3). Cell seeded three types of scaffolds were transferred to new 24-well plate prior to do the Live/Dead cell assay. Cell viability was determined by the use of a green fluorescence dye, calcein, and dead cells were shown through the use of a red fluorescence dye ethidium homodimer-1. Cell viability on scaffolds were imaged using a fluorescence microscope.

Statistical Analysis

For porosity and mechanical testing of scaffolds (n=7 scaffolds per group) were used and the mean \pm standard error was calculated and plotted in the graphs. The IBM SPSS Statistics version 21 software was used to compare porosity and compressive modulus data of the three scaffold groups using one-way analysis of variance (ANOVA) with 99.9% confidence interval followed by Tukey Post Hoc multiple statistical comparison procedure. Differences were considered significant if $p < 0.001$.

ACKNOWLEDGEMENT

The first author would like to thank the University of Toledo for allowing him to use the facilities to conduct the experiments in this project.

Received: July 26, 2018

Accepted: January 18, 2018

Published: April 26, 2019

REFERENCES

1. Pollak, A. N. "Timing of debridement of open fractures." *Journal of the American Academy of Orthopaedic Surgeons*, vol. 14, no. supplement 10, 2006, pp. S48-51.
2. Clarke, B. "Normal bone anatomy and physiology." *Clinical Journal of the American Society of Nephrology*, vol. 3, no. supplement 3, 2008, pp. S131-39.
3. Giannotti, S., *et al.*, "Current medical treatment strategies concerning fracture healing." *Clinical Cases in mineral and bone metabolism*, vol. 10, no. 2, 2013, pp. 116-20.
4. Kon, E., *et al.*, "Bone regeneration with mesenchymal stem cells." *Clinical Cases in mineral and bone metabolism*, vol. 9, no. 1, 2012, pp. 24-27.
5. Seitz, H., *et al.*, "Three-dimensional printing of porous ceramic scaffolds for bone tissue engineering." *Journal of Biomedical Materials Research Part B*. vol. 74, no. 2, 2005, pp. 782-88.

6. Jones, A. C., *et al.*, "Assessment of bone ingrowth into porous biomaterials using MICRO-CT." *Biomaterials*, vol. 28, no. 15, 2007, pp. 2491-04.
7. Burge, R., *et al.*, "Incidence and economic burden of osteoporosis-related fractures in the United States, 2005-25." *Journal of Bone and Mineral Research*, vol. 22, no. 3, 2007, pp. 465-75.
8. De Long, W. G., *et al.*, "Bone grafts and bone graft substitutes in orthopaedic trauma surgery. A critical analysis." *Journal of bone and joint surgery. American volume*, vol. 89, 2007, pp. 649-58.
9. Khan, Y., *et al.*, "Tissue engineering of bone: Material and matrix considerations." *Journal of bone and joint surgery. American volume*, vol. 90, no. supplement 1, 2008, pp. 36-42.
10. Boyce, T., *et al.*, "Allograft bone. The influence of processing on safety and performance." *Orthopedic Clinics of North America*, vol. 30, no. 4, 1999, pp. 571-81.
11. Khademhosseini A., *et al.*, "Progress in tissue engineering." *Scientific American*, vol. 300, no. 5, 2009, pp. 64-71.
12. Bose, S., *et al.*, "Bone tissue engineering using 3D printing." *Materials Today*. vol. 16, no. 12, 2013, pp. 496-04.
13. Misra, S. K., *et al.*, "Poly(3-hydroxybutyrate) multifunctional composite scaffolds for tissue engineering applications." *Biomaterials*, vol. 31, no. 10, 2010, pp. 2806-15.
14. Vergnol, G., *et al.*, "In vitro and in vivo evaluation of a polylactic acid-bioactive glass composite for bone fixation devices." *Journal of Biomedical Materials Research Part B*, vol. 104, no. 1, 2016, pp. 180-91.
15. Zhou, Z., *et al.*, "Development of three-dimensional printing polymer-ceramic scaffolds with enhanced compressive properties and tuneable resorption." *Materials Science and Engineering C*, vol. 93, 2018, pp. 975-86.
16. Rezwana, K., *et al.*, "Biodegradable and bioactive porous polymer inorganic composite scaffolds for bone tissue engineering." *Biomaterials*, vol. 27, no. 18, 2006, pp. 3413-31.
17. Karageorgiou, V., and Kaplan, D. "Porosity of 3D biomaterial scaffolds and osteogenesis." *Biomaterials*, vol. 26, no. 27, 2005, pp. 5474-91.
18. Jeong, C. G., and Atala, A. "3D Printing and Biofabrication for Load Bearing Tissue Engineering." *Advances in Experimental Medicine and Biology*, vol. 881, 2015, pp. 3-14.
19. Hollister, S. J., *et al.*, "Design control for clinical translation of 3D printed modular scaffolds." *Annals of Biomedical Engineering*, vol. 43, no. 3, 2015, pp. 774-86.
20. Li, Z., and Tan, B. H. "Towards the development of polycaprolactone based amphiphilic block copolymers: molecular design, self-assembly and biomedical applications." *Materials Science and Engineering C*, vol. 45, 2014, pp. 620-34.
21. Woodruff, M. A., and Hutmacher, D. W. "The return of a forgotten polymer-Polycaprolactone in the 21st century." *Progress in Polymer Science*. vol. 35, no. 10, 2010, pp. 1217-56.
22. Williams, J. M., *et al.*, "Bone tissue engineering using polycaprolactone scaffolds fabricated via selective laser sintering". *Biomaterials*, vol. 26, no. 23, 2005, pp. 4817-27.
23. Cahill, S., *et al.*, "Finite element predictions compared to experimental results for the effective modulus of bone tissue engineering scaffolds fabricated by selective laser sintering." *Journal of Materials Science: Materials in Medicine*, vol. 20, no. 6, 2009, pp. 1255-62.
24. Bose, S., *et al.*, "Recent advances in bone tissue engineering scaffolds." *Trends in Biotechnology*, vol. 30, no. 10, 2012, pp. 546-54.
25. Olszta, M. J., *et al.*, "Bone structure and formation: A new perspective." *Materials Science & Engineering R: Reports*, vol. 58, no. 3-5, 2007, pp. 77-116.
26. Petrigliano, F. A., *et al.*, "In vivo evaluation of electrospun polycaprolactone graft for anterior cruciate ligament engineering." *Tissue Engineering Part A*, vol. 21, no. 7-8, 2015, pp. 1228-36.
27. Nyitray, C. E., *et al.*, "Polycaprolactone Thin-Film Micro- and Nanoporous Cell-Encapsulation Devices." *ACS Nano*. vol. 9, no. 6, 2015, pp. 5675-82.
28. Williams, D. F. "On the mechanisms of biocompatibility". *Biomaterials*, vol. 29, no. 20, 2008, pp. 2941-2953.
29. Sun, H., *et al.*, "The in vivo degradation, absorption and excretion of PCL-based implant". *Biomaterials*, vol. 27, no. 9, 2006, pp. 1735-40.